

## ***In situ* second harmonic generation studies of bisulfate adsorption at well-ordered Pt(111) and Pt(100) electrodes**

ML Lynch, BJ Barner, JM Lantz, RM Corn

*Department of chemistry, University of Wisconsin, 1101 University Ave, Madison, WI 53706 USA*

### **Abstract :**

The technique of optical second harmonic generation (SHG) is used to monitor bisulfate chemisorption at well-ordered Pt(111) and Pt(100) electrodes in perchloric acid media. A comparison of the surface SHG response from the well-ordered single crystal electrodes to that obtained from polycrystalline platinum electrodes indicates that at potentials positive of hydrogen adsorption a limited amount of bisulfate chemisorption inhibits and suppresses the other electrochemical surface reactions. Upon disordering, the amount of bisulfate chemisorption increases towards the levels observed at polycrystalline surfaces.

La technique de la génération optique du 2ème harmonique (SHG) est utilisée pour suivre la chimisorption du bisulfate sur des électrodes bien ordonnées de Pt(111) et Pt(100) en milieu acide perchlorique. La comparaison des réponses SHG sur surfaces monocristallines et sur surface polycristalline indique qu'à des potentiels positifs par rapport à l'adsorption de l'hydrogène une quantité limitée de bisulfate chimisorbé inhibe et supprime les autres réactions électrochimiques de surface. Lorsque la surface devient désorganisée, la quantité de bisulfate chimisorbé augmente pour tendre vers la valeur observée sur surface polycristalline.



### I. Introduction

Detailed mechanistic studies of surface reactions at solid metal electrodes are typically performed at single crystal electrodes in order to insure that the metal surface consists of a homogenous, reproducible number of reaction sites to which the surface reactivity can be related. The observation that the electrochemical activity of the Pt(111) surface also depends upon the long-range order of the surface [1,2] demonstrated that surface reactivity relies not only upon the local configuration of the reactants and products at the surface, but also upon the ordered adsorption of the interfacial species participating in the reaction.

Concurrently, *in situ* measurements at gold single crystal surfaces have shown that surface reconstruction will occur as a function of electrode potential and the presence of various chemisorbed species [3,4]. These studies furthered the realization that the long range order of the surface itself was intimately tied to the extent and type of chemisorption occurring at the interface. For these reasons it is of great interest to develop and employ a wide variety of non-electrochemical methods to monitor the ordered structures that can appear upon chemisorption onto single crystal electrodes. Various groups have been involved in both *ex situ* [5-9] and *in situ* [10-14] studies of electrochemical interfaces to this end. In a recent series of papers [15-19] we utilized optical second harmonic generation (SHG) as an *in situ* probe for ordered chemisorption and structure at platinum electrodes in perchloric acid solutions.

This paper extends those SHG measurements to the *in situ* study of bisulfate chemisorption at Pt(111) and Pt(100) electrochemical surfaces. Bisulfate chemisorption has been monitored previously with SHG at polycrystalline platinum electrodes [15]. The adsorption of bisulfate at well-ordered and disordered Pt(111) and Pt(100) electrodes can be examined by noting the changes

in the surface SHG response upon addition of bisulfate to the perchloric acid medium. For well-ordered Pt(111) surfaces, a limited amount of bisulfate is found to chemisorb onto the electrode at potentials positive of the anomalous voltammetric waves originally observed by Clavilier [1]. This bisulfate adsorption suppresses the other adsorption processes that are observed in the absence of bisulfate. Upon disordering of the Pt(111) surface, the amount of bisulfate chemisorption increases to the levels observed on polycrystalline surfaces; similar effects are observed on the Pt(100) electrode. Anisotropy measurements on the Pt(111) electrode confirm that the various nonlinear susceptibility surface tensor elements are changing upon chemisorption of bisulfate, iodine, CO and hydrogen onto the surface.

### II. Theory

The second order nonlinear optical response from the platinum-water interface arises from an electric dipole allowed contribution from the metal surface and higher order contributions from the bulk metal [10,15,20,21]. The second harmonic intensity  $I(2\omega)$  from the interface is proportional to the square of its complex nonlinear susceptibility  $\chi$ :

$$I(2\omega) \propto | \mathbf{e}(2\omega) \cdot \chi \cdot \mathbf{e}(\omega) \mathbf{e}(\omega) |^2 I^2(\omega) \quad (1)$$

where  $I(\omega)$  is the input light power and  $\mathbf{e}(\omega)$  and  $\mathbf{e}(2\omega)$  are polarization vectors describing the input and output light fields [18]. Since  $\chi$  relates two input vectors to one output vector, it is a third rank tensor and in general can have 18 distinct nonzero complex elements,  $\chi_{ijk}$ . For most systems, the number of nonzero elements is greatly reduced by the surface symmetry [21]. For polycrystalline and Pt(100) electrodes, the surface contributions to the nonlinear susceptibility can be described by three independent tensor elements:  $\chi_{ZZZ}$ ,  $\chi_{ZXX}$ , and  $\chi_{XXZ}$  where Z



is defined as the surface normal. For Pt(111) electrodes, a fourth independent surface tensor element,  $\chi_{XXX}$ , exists.

The nonlinear susceptibility of an electrode surface can be described as the sum of three possible sources:

$$\chi = \chi_S + \chi_A + \chi_I \quad (2)$$

where  $\chi_S$  is the nonlinear susceptibility of the platinum substrate (including the higher order bulk terms) in the absence of adsorption,  $\chi_A$  is the inherent nonlinear susceptibility of the species adsorbed onto the surface, and  $\chi_I$  is the change in the nonlinear susceptibility of the platinum surface and adsorbate due to any surface-adsorbate interactions. For the wavelengths employed in this study,  $\chi_S$  is typically larger than  $\chi_A$  for the monatomic hydrogen, oxide, and bisulfate adsorbates. However, the changes in the nonlinear optical response upon adsorption ( $\chi_I$ ) are large enough to permit the detection of submonolayer quantities of these adsorbates. This indirect monitoring of chemisorption is called "nonresonant SHG" in reference to the fact that the optical properties of the metal do not in general change rapidly with wavelength. On a variety of platinum surfaces, the changes in the nonresonant SHG with potential have been used previously to indirectly monitor the chemisorption of species [15, 17-19].

To probe the various surface tensor elements of the platinum electrodes, one measures the SHG response of the surface for a series of input and output polarizations as a function of azimuthal angle [10, 19, 21]. For the Pt(111) surface the azimuthal angle  $\phi$  is defined as the angle between the [2,-1,-1] crystal axis and the projection of the input light vector on the surface. In this paper we will restrict ourselves to the potential dependence of  $I_{p,p}(2\omega)$  and  $I_{s,p}(2\omega)$  and to anisotropy measurements of  $I_{s,p}(2\omega)$  on the Pt(111) surface, where the subscript's

of the SHG signal  $I_{input,output}(2\omega)$  refer to polarization of the incident (input) and second harmonic (output) light fields [ $s = s$ -polarized light and  $p = p$ -polarized light]. The potential dependence of  $I_{p,p}(2\omega)$  reflects changes in the susceptibility tensor elements  $\chi_{ZZZ}$ ,  $\chi_{XXX}$  and  $\chi_{XXZ}$  as the state of chemisorption on the surface is varied. The  $\phi$ -dependence of the SHG response reflects the average symmetry of the bulk, surface, and adsorbate contributions to the nonlinear susceptibility. For the Pt(111) surface, the azimuthal dependence of the  $I_{s,p}(2\omega)$  signal can be written as [19]:

$$I_{s,p}(2\omega) = |a_{s,p} + c_{s,p} \cos(3\phi)|^2 \quad (3)$$

where the complex constants  $a_{in,out}$  and  $c_{in,out}$  are combinations of bulk and surface contributions to  $\chi$  multiplied by the incident laser power and the Fresnel coefficients at the incident and second harmonic wavelengths [19]. For the Pt(111) surface, the constant  $c_{s,p}$  is related to the tensor element  $\chi_{XXX}$ , whereas  $a_{s,p}$  is a measure of the  $\chi_{ZZZ}$ . No anisotropy is expected from the polycrystalline and unreconstructed Pt(100) surfaces.

### III. Experimental Considerations and Sample Preparation

The SHG signal at 302 nm measured in these experiments was created at the electrode surface from a 604 nm pulsed laser at an incident angle of 60° with respect to the surface normal. The SHG signal was obtained with a photon counting system normalized by a separate reference channel and is expressed in counts  $s^{-1}$ , each point of the SHG response was obtained with 1 second of integration time (or 4 million laser pulses). The  $I_{p,p}(2\omega)$  and  $I_{s,p}(2\omega)$  polarized SHG measurements were obtained with Glan-Laser polarizers (Special Optics); the polarizers were verified to have extinction ratios of  $10^{-5}$  or better at the two



wavelengths. Further details of the experimental apparatus are published elsewhere [18].

The well-ordered platinum electrodes were prepared by flame annealing followed by the iodine/CO exchange method developed by Zurawski et al. [22,23]. The electrodes employed in the experiments were either a 6 mm polycrystalline 99.99% platinum (Johnson Matthey) rod, a 6 mm polished Pt(111) crystal (Arenco), or a 1 cm diameter polished Pt(100) crystal (Johnson-Matthey). The crystal axes for the single crystals were determined by Laue backscattering diffraction measurements. Prior to the immersion of the electrode, the single crystals were heated to 800°C in a hydrogen flame and then cooled in an argon/iodine vapor stream to allow for the dissociative chemisorption of iodine onto the surface. The electrodes were then mounted onto a glass rod, sealed around the edge with teflon tape, and immersed into a two window spectroelectrochemical cell [15]. The electrode potential was controlled by a Princeton Applied Research 173/175 potentiostat; all potentials are reported versus a SCE(Sat'd NaCl) reference that was isolated from the main solution. The cell contained approximately 70 ml of a 0.1M HClO<sub>4</sub> (doubly-distilled from Vycor GFS Chemicals) solution prepared from water that was Millipore-filtered and then doubly distilled. The electrode was exposed to a saturated CO solution in order to displace the iodine from the surface with an adsorbed CO monolayer.

The CO saturated solution was then replaced with either a clean perchloric acid solution or a perchoric acid solution with 1 mM sulfuric acid (puris pa grade from Fluka). [Note: At the pH employed in these experiments the predominant sulfate species is bisulfate; therefore the chemisorption will be described as bisulfate chemisorption, although it is possible (and likely) that the chemisorption of sulfate ions also occurs.] The CO was removed from the surface by

electrochemical oxidation to CO<sub>2</sub>, resulting in the cyclic voltammogram (CV) of a well-ordered single crystal surface. The potential dependence of the  $I_{p,p(2\omega)}$  and  $I_{s,p(2\omega)}$  were recorded simultaneously with the CV at a scan rate of 20 mV s<sup>-1</sup>. Anisotropy measurements of  $I_{s,p(2\omega)}$  for the Pt(111) surface were obtained by holding the potential and rotating the electrode about the surface normal.

#### IV. Results and Discussion

##### A. Perchloric Acid Solutions

Figure 1 depicts the CV and the  $I_{p,p(2\omega)}$  SHG response as a function of electrode potential from polycrystalline platinum, Pt(111) and Pt(100) electrodes in 0.1M perchloric acid. The CV of the polycrystalline platinum surface (Figure 1a) exhibits the familiar double layer, oxide formation and hydrogen deposition potential regions [5]. On this electrode the SHG response increases quantitatively with the adsorption of monatomic hydrogen onto the electrode [15]. Throughout the rest of the CV the signal level remains relatively low, indicating that there is little change in the SHG response with changes in the DC electrostatic fields at the surface and upon oxide formation.

The CV and  $I_{p,p(2\omega)}$  SHG response from the Pt(111) electrode is shown in Figure 1b. The voltammetry originally reported by Clavilier [1,2] for the hydrogen and oxygen electroreduction processes at this electrode differs markedly from the polycrystalline case. Three major conclusions have been reached by various authors concerning the Pt(111) electrode: (i) there is a long range ordering process that is responsible for the unusual voltammetry, (ii) the deposition of atomic hydrogen is quite different on the well-ordered Pt(111) surface as compared to disordered Pt(111) and polycrystalline electrodes, and (iii) at positive potentials there appears to be the formation of OH and other oxide species that are not



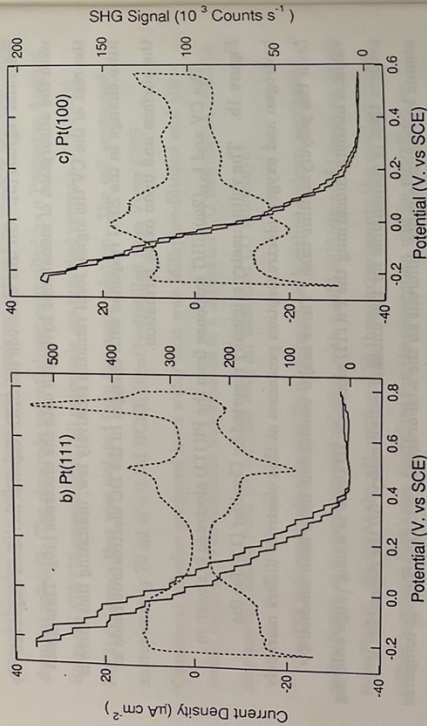
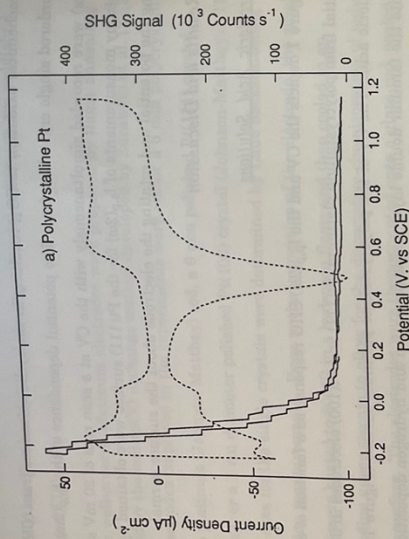


Figure 1. Cyclic voltammetry (dashed line) and potential dependence of the  $I_{p,p}(2\omega)$  surface SHG response (solid line) in 0.1M perchloric acid from: (a) polycrystalline Pt, (b) Pt(111) oriented with  $\phi=30^\circ$ , (c) Pt(100). The scan rate is 20 mV/sec.

observed on disordered Pt(111) and polycrystalline electrodes [24-26]. As described previously [19], the  $I_{p,p}(2\omega)$  SHG signal increases linearly and reversibly at potentials negative of 0.400 V following the broad "capacitive wave" on the shoulder of the sharp, reversible "butterfly peaks" at 0.490 V. A comparison to the polycrystalline electrodes suggests that this rise in signal is due to the adsorption of a hydrogen species perturbing the nonlinear optical response of the platinum surface. For Pt(100) electrodes (Figure 1c) a substantial rise in the SHG signal is once again seen at potentials for which there is an adsorbed layer of monatomic hydrogen.

It is interesting to note that for Pt(111) the SHG signal increases throughout the region where there is no current, implying that there are changes occurring in the electronic structure of the surface in the absence of any faradaic adsorption processes. Although the  $I_{p,p}(2\omega)$  SHG response rises without break for all potentials negative of 0.400 V, the potential dependence of the  $I_{p,p}(2\omega)$  SHG response from the Pt(111) electrode (Figure 2a) exhibits a different second harmonic response positive and negative of the hydrogen waves at 0 V. This change in the  $I_{p,p}(2\omega)$  SHG response suggests that the species adsorbed onto the surface from 0 V to 0.400 V alters the surface electronic structure in a different manner than the adsorbed hydrogen at more negative potentials. Since the nonresonant SHG signal is an indirect probe of chemisorption, it is unfortunately impossible to be more specific as to the nature of this adsorbed species.

At potentials positive of hydrogen adsorption, the  $I_{p,p}(2\omega)$  SHG response in Figure 2a correlates with the other features observed on the Pt(111) voltammetry. The  $I_{p,p}(2\omega)$  SHG signal rises twice, first during the sharp butterfly peaks, and a second time after the irreversible peak in the CV at 0.730 V. Other authors have attributed these features in the voltammetry to formation of OH and oxide species



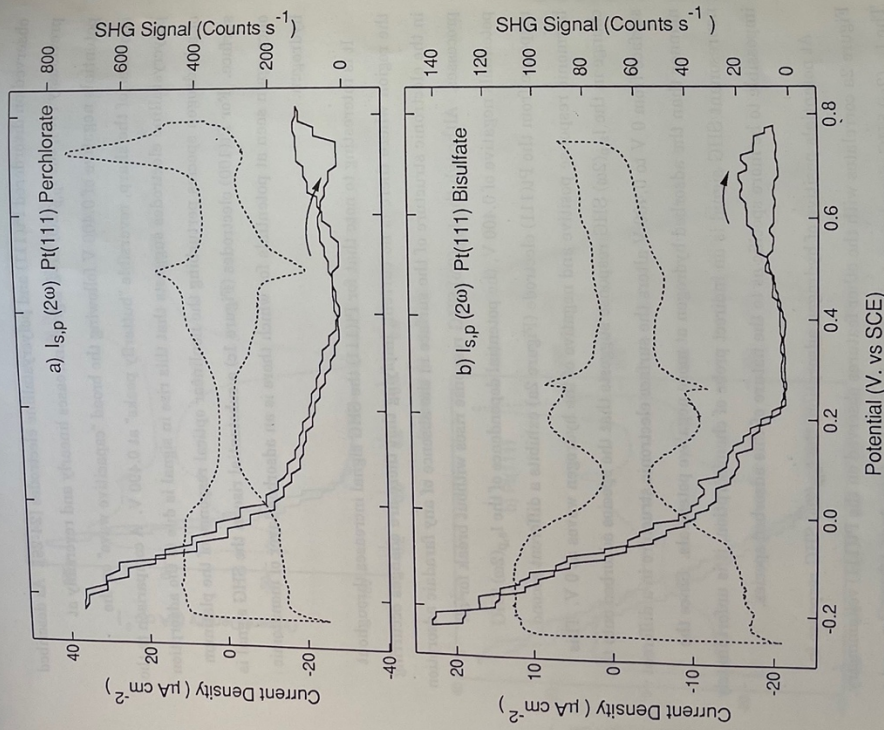


Figure 2. Cyclic voltammetry (dashed line) and potential dependence of the  $I_{s,p}(2\omega)$  surface SHG response (solid line) from a Pt(111) surface oriented with  $\phi=30^\circ$  in (a) 0.1M perchloric acid, (b) 0.1M perchloric acid + 1 mM sulfuric acid.

on the surface [24]. The  $I_{s,p}(2\omega)$  SHG signal demonstrates that these faradaic reactions are indeed due to surface processes.

B. Sulfuric Acid Solutions

Figure 3 plots the CV and potential dependence of the  $I_{p,p}(2\omega)$  SHG response for the three platinum electrodes in the presence of 1 mM bisulfate. For the polycrystalline surface (Figure 3a), a rise in the SHG signal is observed throughout the double layer region. This rise has been used previously to obtain the relative amount of chemisorbed bisulfate on the surface; the potential dependence of this relative surface coverage measurement agrees with the results of radiotracer adsorption experiments [27]. The amount of bisulfate chemisorption depends upon the solution concentration of bisulfate; by 1 mM the amount of chemisorption has reached its maximum value. Slight changes are observed in the hydrogen and oxide electrochemistry, but for the most part the chemisorption occurs in the double layer region and does not strongly influence the faradaic processes.

In contrast, the well-ordered Pt(111) electrochemistry is radically altered in the presence of bisulfate. Large changes in the voltammetry are observed in the oxide and butterfly regions of the CV (Figure 3b). Using the potential dependence of the  $I_{s,p}(2\omega)$  and  $I_{p,p}(2\omega)$  SHG signals (Figures 2b and 3b respectively), it is clear that these changes are due to the chemisorption of bisulfate competing with the other surface processes. The increase in the  $I_{p,p}(2\omega)$  SHG signal positive of the butterfly peaks is reminiscent of that observed due to bisulfate adsorption on polycrystalline surfaces. However, the magnitude of the chemisorption response is much less than that on polycrystalline platinum, either due to changes in the nature of the chemisorption on the Pt(111) surface or to a decrease in the amount of bisulfate



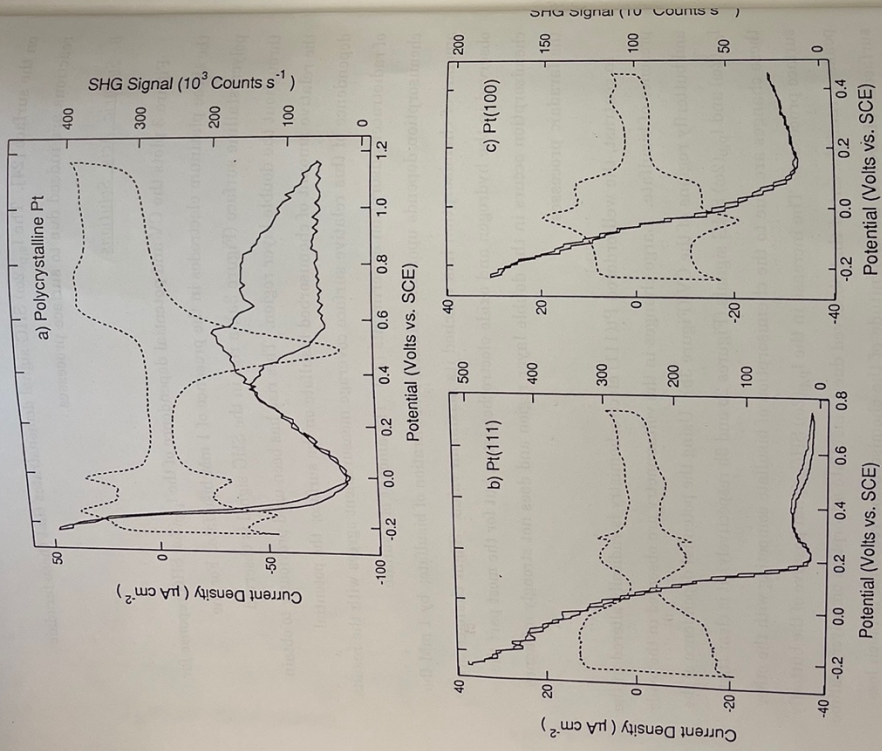


Figure 3. Cyclic voltammetry (dashed line) and potential dependence of the  $I_{p,p}(2\omega)$  surface SHG response (solid line) in 0.1M perchloric acid + 1 mM sulfuric acid from: (a) polycrystalline Pt, (b) Pt(111) oriented with  $\phi=30^\circ$ , (c) Pt(100).

chemisorption on the surface. The  $I_{s,p}(2\omega)$  potential dependence also demonstrates that the OH and oxide surface processes mentioned above are absent in the presence of bisulfate. As in the case of polycrystalline platinum electrodes, oxide formation eventually forces the bisulfate species to desorb and results in irreversible changes in the  $I_{s,p}(2\omega)$  signal at potentials positive of 0.600 V.

At potentials negative of the anomalous hydrogen wave for Pt(111) in the presence of bisulfate, the  $I_{p,p}(2\omega)$  and  $I_{s,p}(2\omega)$  SHG signals increase due to the adsorption of a hydrogen species much as in the case of perchlorate media (except that the potentials are shifted by -0.230 V). Note that the SHG signal does not begin to rise until well into the capacitive wave on both the positive and negative scans. This result suggests that the adsorption processes responsible for the sharp butterfly peak are not the same as the adsorption processes which are related to the capacitive wave.

Figure 3c plots the CV and the potential dependence of the  $I_{p,p}(2\omega)$  SHG signal from Pt(100) electrodes in the presence of 1mM bisulfate. In both curves there is little to indicate the presence of bisulfate adsorption. At potentials positive of the hydrogen waves there is a small, reversible linear increase in SHG signal that can be attributed to the adsorption of bisulfate, but at a much lower level than that observed on polycrystalline electrodes. At potentials negative of 0.100 V the chemisorption of hydrogen leads to an increase the SHG signal similar to that observed in the absence of bisulfate.

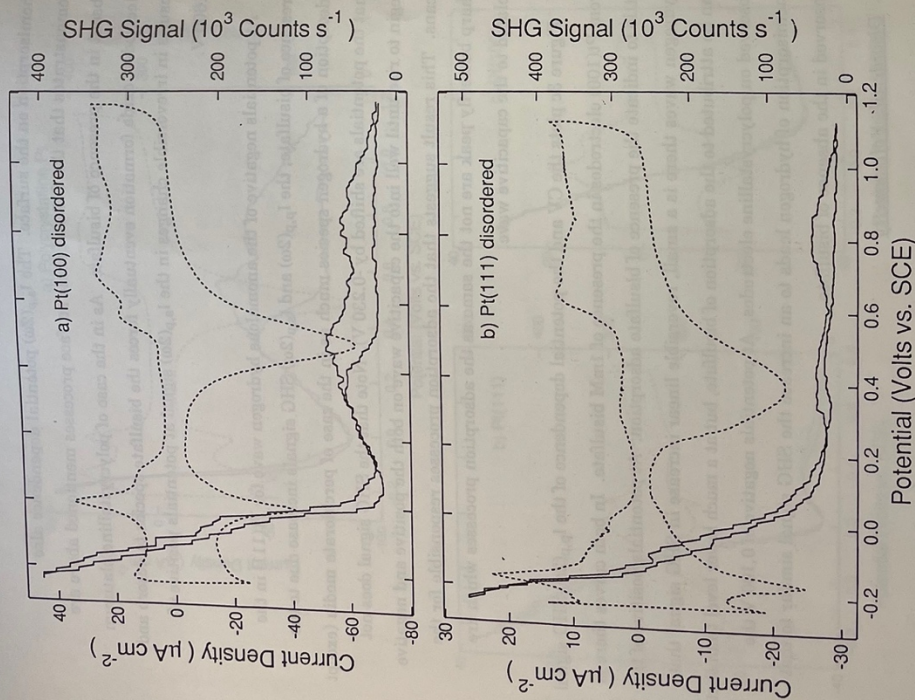
C. Disordered Voltammetry

Figure 4 plots the disordering of the Pt(111) and Pt(100) surfaces in the presence of bisulfate by scanning to positive potentials. This disordering never



leads to a surface that exhibits the electrochemistry of a polycrystalline electrode, and is therefore denoted as "disordered Pt(111)" and "disordered Pt(100)". For the disordered Pt(100) surface, oxide formation occurs at potentials positive of 0.600 V on the anodic sweep, followed by the characteristic oxide removal peak at 0.450V (Figure 4a). In the hydrogen region, the peak observed in the ordered Pt(100) remains and can be identified with the "strongly adsorbed" hydrogen peak at 0 V in the polycrystalline CV (Figure 1a). After a single cycle, the  $I_{p,p}(2\omega)$  SHG signal was found to change to a response similar to that observed from polycrystalline electrodes: an increase is observed in both the hydrogen and double layer regions due to the chemisorption of monatomic hydrogen and bisulfate respectively. This increase in  $I_{p,p}(2\omega)$  throughout the double layer region suggests that the disordering of the Pt(100) surface has enhanced the amount of chemisorption occurring in the double layer region.

The voltammetry and  $I_{p,p}(2\omega)$  SHG response from the disordered Pt(111) surface are shown in Figure 4b. Unlike the Pt(100) surface, the changes in the CV and SHG signal do not occur after a single positive scan, but only reach a steady state after many oxidation-reduction cycles. At positive potentials, the CV once again shows the characteristic oxide formation and removal waves of the polycrystalline surface. In the hydrogen region, the butterfly peaks disappear and the growth of a peak at -0.170 V from the continuous hydrogen waves on the ordered surface is observed; this peak can be associated with the "weakly adsorbed" hydrogen peak in the polycrystalline voltammetry [5,28]. The  $I_{p,p}(2\omega)$  SHG signal from the disordered Pt(111) surface changes concurrently with the changes observed in the CV; the increase in the  $I_{p,p}(2\omega)$  SHG signal in the hydrogen region is no longer monotonic and rises sharply at the potential of the new hydrogen peak. The  $I_{p,p}(2\omega)$  SHG signal at potentials positive of 0.100 V



**Figure 4.** Cyclic voltammetry (dashed line) and potential dependence of the  $I_{p,p}(2\omega)$  surface SHG response (solid line) during surface disordering in 0.1M perchloric acid + 1 mM sulfuric acid of (a) Pt(100), (b) Pt(111) oriented with  $\phi=30^\circ$ .



decreases as the butterfly peaks decrease with repeated cycling, and after many cycles resembles the SHG signal due to bisulfate adsorption observed on Pt(100) and polycrystalline surfaces. This SHG signal is still diminished in magnitude, however, and suggests that even on the disordered Pt(111) surface there is still an inhibition of bisulfate chemisorption, perhaps due to the presence of another species that does not contribute to the surface SHG response.

#### D. SHG anisotropy measurements

Although the potential dependence of the  $I_{s,p}(2\omega)$  and  $I_{s,p}(2\omega)$  SHG signals are sufficient to demonstrate the presence of the various chemisorbed species on platinum electrodes, a more accurate measure of the changes to the surface nonlinear susceptibility tensor upon chemisorption can be made through rotational anisotropy studies of the surface at fixed potentials [10,19,20,29]. To emphasize the changes observed in the second harmonic response upon the chemisorption of species onto the Pt(111), Figure 5 shows the  $I_{s,p}(2\omega)$  anisotropy for four different chemisorbed species at various potentials: iodine, CO, bisulfate, and hydrogen. The anisotropies are plotted in polar coordinates with the x axis corresponding to the [2,-1,-1] crystal axis. All of the anisotropy plots can be fit to Equation 3 with different magnitudes and phases for the constants  $a_{s,p}$  and  $c_{s,p}$ . Although higher order contributions from the first 10 nm of the bulk Pt crystal can in principle contribute to the  $I_{s,p}(2\omega)$  anisotropy [21], the large changes in the magnitude and phase of the anisotropy plots from the Pt(111) electrode in Figure 5 attest to the sensitivity of the SHG signal to chemisorption processes on that surface. A quantitative discussion of the changes in the anisotropy plots will be presented in a subsequent paper.

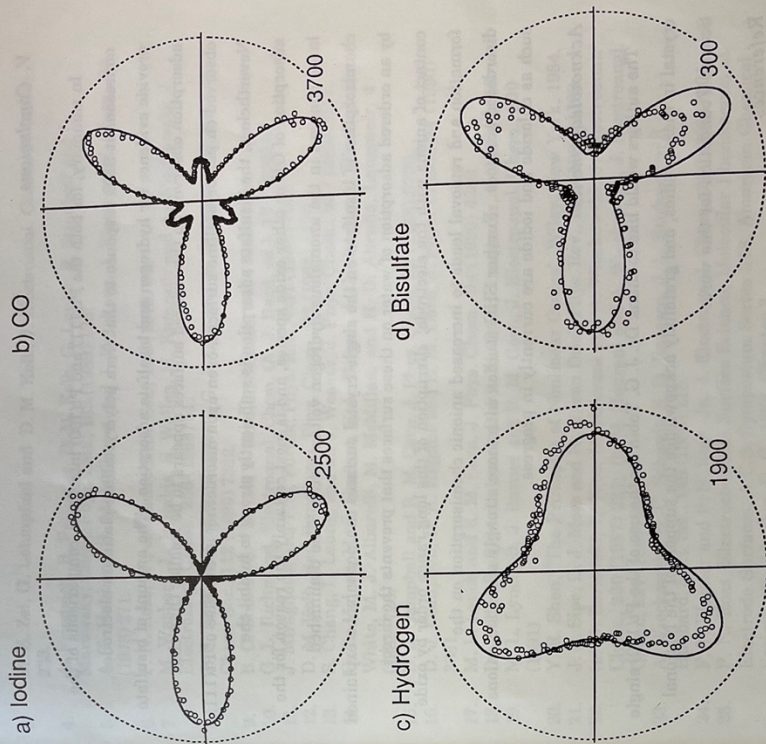


Figure 5. Polar plots of  $I_{s,p}(2\omega)$  as a function of azimuthal angle  $\phi$  for Pt(111) with an adsorbate: (a) iodine monolayer in 0.1M perchloric acid at 0.200V, (b) CO monolayer in 0.1M perchloric acid at 0.200V, (c) monatomic hydrogen monolayer in 0.1M perchloric acid + 1 mM sulfuric acid at -0.200V, and (d) bisulfate monolayer in 0.1M perchloric acid + 1 mM sulfuric acid at 0.350V. The x-axis in the polar plot corresponds to  $\phi=0^\circ$ , and the solid lines are fits to Equation 3. The circles in each plot correspond to a constant SHG signal that is given in counts/sec.



### V. Conclusions

In summary, for both the Pt(111) and Pt(100) interfaces, comparisons of the nonresonant SHG response to that from polycrystalline platinum electrodes provide evidence for hydrogen and bisulfate adsorption. The amount of bisulfate adsorption observed on the ordered surfaces appears to be smaller than that observed on polycrystalline surfaces, even upon disordering in the case of Pt(111). Nevertheless, the bisulfate adsorption is sufficiently strong to inhibit the adsorption of OH or other oxide species, and is most certainly the reason for the large changes in the anomalous hydrogen voltammetry. The diminished chemisorption of bisulfate on the single crystal surfaces can perhaps be explained by an ordered adsorption of water on these surfaces that prevents the direct contact of anions with the electrode; disruption of this long range order by oxide formation and removal leads to increased anionic chemisorption on the disordered surfaces. Further SHG studies with more strongly adsorbed anions such as chloride and iodide are currently in progress.

### Acknowledgements

The authors would like to thank Dr. J. G. Tobin for the use of the Pt(100) single crystal in these studies, and gratefully acknowledge the support of the National Science Foundation for this work.

### References

1. (a) J. Clavilier, R. Faure, G. Guinet and R. Durand, *J. Electroanal. Chem.*, **107** (1980) 205; (b) J. Clavilier, *J. Electroanal. Chem.*, **107** (1980) 211.
2. (a) C. L. Sorehimi and C. N. Reilley, *J. Electroanal. Chem.*, **139** (1982) 247; (b) S. Motoo and N. Furuya, *J. Electroanal. Chem.*, **172** (1984) 339.

3. M. S. Zei, G. Lehmppfuhl and D. M. Kolb, *J. Electroanal. Chem.*, **96** (1979) 233.
4. A. Friedrich, B. Pettinger, D. M. Kolb, G. Lupke, R. Stienhoff and G. Marowsky, *Chem. Phys. Lett.*, **163** (1989) 123.
5. A. T. Hubbard, R. M. Ishikawa and J. Katakari, *J. Electroanal. Chem.*, **86** (1978) 271.
6. P. N. Ross, Jr., *J. Electrochem. Soc.*, **126** (1979) 67.
7. M. Wasberg, L. Palaiakis, S. Wallen, M. Kamrath and A. Wieckowski, *J. Electroanal. Chem.*, **256** (1988) 51.
8. J. F. Rodriguez, M. E. Bothwell, G. J. Call and M. P. Soriaga, *J. Am. Chem. Soc.*, **112** (1990) 7392.
9. B. C. Shardt, S. Yau and F. Rinaldi, *Science*, **243** (1989) 1050.
10. G. L. Richmond, *Electroanal. Chem. (A. J. Bard, ed.)*, **17** (1990) 87.
11. J. Miraghiota and T. E. Furtak, *Phys. Rev.*, **B37** (1988) 1028.
12. D. M. Kolb, *Ber. Bunsenges. Phys. Chem.*, **92** (1988) 1175.
13. S. Chang, L. Leung, and M. J. Weaver, *J. Phys. Chem.*, **93** (1989) 5341.
14. O. R. Melroy, M. G. Samant, G. L. Borges, J. G. Gordon, L. Blum, J. H. White, M. J. Albarelli, M. McMillan, and H. D. Abruna, *Langmuir*, **4** (1988) 728.
15. D. J. Campbell and R. M. Corn, *J. Phys. Chem.*, **92** (1988) 5796.
16. D. J. Campbell, D. A. Higgins and R. M. Corn, *J. Phys. Chem.*, **94** (1990) 3681.
17. M. L. Lynch and R. M. Corn, *J. Phys. Chem.*, **94** (1990) 4382.
18. D. J. Campbell, M. L. Lynch and R. M. Corn, *Langmuir*, **6** (1990) 1656.
19. M. L. Lynch, B. J. Barner and R. M. Corn, *J. Electroanal. Chem.*, **300** (1991).
20. Y. R. Shen, "The Principles of Nonlinear Optics", Wiley, New York, 1984.
21. J. E. Sipe, D. J. Moss and H. M. van Driel, *Phys. Rev.*, **B35** (1987) 1129.
22. (a) D. Zurawski, L. Rice, M. Hourani and A. Wieckowski, *J. Electroanal. Chem.*, **230** (1987) 221; (b) M. Hourani and A. Wieckowski, *J. Electroanal. Chem.*, **227** (1987) 257.
23. A. Wieckowski, B. C. Shardt, S. D. Rosasco, J. L. Stackney and A. Hubbard, *Surf. Sci.*, **146** (1984) 115.
24. F. T. Wagner and P. N. Ross, Jr., *J. Electroanal. Chem.*, **250** (1988) 301.
25. P. N. Ross, *Electrochemical Surface Science, Molecular Phenomenon at Electrode Surfaces*, ACS Symposium Series **378**, American Chemical Society, Washington, D. C., 1988, Chapter 3.
26. K. Al Jaaf-Golze, D. M. Kolb, and D. Scherson, *J. Electroanal. Chem.*, **200** (1986) 353.
27. G. Horyani, J. Solt and G. Vertes, *J. Electroanal. Chem.*, **32** (1971) 271.
28. F. G. Will, *J. Electrochem. Soc.*, **112** (1965) 451.
29. (a) T. A. Driscoll and D. Guidotti, *Phys. Rev.*, **B28** (1983) 1171; (b) H. W. K. Tom, T. F. Heinz and Y. R. Shen, *Phys. Rev. Lett.*, **51** (1983) 1983; (c) T. F. Heinz, M. M. T. Loy and W. A. Thompson, *Phys. Rev. Lett.*, **54** (1985) 63; (d) H. W. K. Tom and G. D. Aumiller, *Phys. Rev.*, **B33** (1986) 8818.